# Mode Harnessing for
# Laser Diodes

Nikolai Stelmakh and Michael Vasilyev

Recent experiments indicate that the modal structure of broad-area edge-emitting semiconductor lasers maintains its behavior under widely varying conditions, with each lateral mode having a distinct wavelength. Thus, researchers can now reshape lateral modes and effectively combine all multimode laser output into a single-mode fiber. This approach provides a promising means for delivering high-power, high-speed modulated beams of any wavelength that are directly radiated from semiconductor lasers.

**L**aser diodes—one of the most efficient coherent light sources—are omnipresent in our everyday life. Their extraordinary efficiency, ease of modulation, robustness and compactness are driving their rapid proliferation in various applications.

Since the demonstration of the first semiconductor laser, researchers have been confronted with the difficult challenge of how to improve laser beam quality. How can we make semiconductor laser output that is powerful enough and, at the same time, spatially coherent enough to be focused into a diffraction-limited spot with the help of a simple lens? There are two obvious ways: to improve the optical strength of laser diode facets (to enable higher output intensity) and to increase the surface area of radiation (to collect this intensity from a larger area).

Due to the delivery of the electrons to the active medium by the p-n junction, one can only increase the radiation surface for edge-emitting lasers by increasing the laser stripe width. Ideally, with the constant refractive index, any stripe width can potentially have a single-mode structure and provide a spatially coherent beam. In reality, however, the refractive index follows the local intensity and temperature, which, in turn, determines the minimum index contrast (and, therefore, the maximum stripe width) for a single-mode operation. This width/single-mode-power trade-off is an important subject of research and development for numerous academic and industrial groups in the world.

The directions that have been pursued so far can be roughly classified as follows: 1) to increase the optical strength of active materials; 2) to increase the output facet area for a single-mode cavity (variable width lasers, MOPA lasers, VCSELs, etc.); 3) to modify the intrinsic single-mode cavity (tilted or curved mirrors, coupled waveguide cavities); 4) to stabilize the single-spatial mode by using an external cavity; 5) to engage in architectural power scaling by external coherent and incoherent (wavelength division multiplexing) combining of laser diode beams; and 6) to convert the beam by a secondary active medium using laser diodes as pumps for rare-earth-doped and Raman fiber lasers, etc.

Since the first telecom lasers were launched in the early 1980s, the optical damage threshold has been pushed up by more than one order of magnitude. However, despite the incredible amount of ingenuity that researchers have already shown, the main technology of single-spatial-mode sources based on semiconductor lasers has remained essentially unchanged. The status quo can be easily summed up by observing that the two high-volume products in today's laser diode industry are single-mode laser diodes that provide single-mode output by narrow (3–5 μm) stripe and broad-area laser diodes that provide multimode light to pump solid-state or fiber lasers.

Thus, today's consensus is to use a narrow-stripe laser for moderate single-mode power applications (<1–5 W) and to use broad-area diode lasers to pump a secondary high-power single-mode laser system for higher-power applications (more than 1-5 W). The diode-pumped solid-state and fiber laser systems have been commercially available for more than a decade, and they represent great research and engineering prowess. However, many applications—including free-space communications, laser micromachining, LADARS, etc.—require high-speed-modulated beams, which are very difficult to produce with high powers. Also, the wavelengths outside of the Nd:YAG and erbium-doped-fiber gain regions are often desirable. Thus, a direct-modulated 10–100 W diode laser source would be a great solution. Why is it still considered impossible to use a modern broad-area laser diode with 10–100 W of output power as a single-mode source?

This question motivated us to revisit the old problem of combining the modes of broad-area lasers. Recent insights into the diode laser mode structure, and significant progress in optical fabrication techniques and optical materials during the telecom revolution of 1998 to 2002, suggest that the broad-area laser with single-mode output idea may work—but in a way that is quite different from previous efforts. Instead of forcing the multi-mode laser into the single-mode regime that is prone to huge instabilities due to nonlinear mode coupling, the broad-area semiconductor laser would be allowed to run in its natural high-efficiency, spatially multi-mode regime.

An external linear optical system separates all modes in a spectral plane and then individually modifies the shape of each mode using a system of phase masks. Finally, it recombines the radiation into a multi-longitudinal but spatially single-mode (i.e., diffraction-limited) spot. Early experiments to combine simultaneously 400 lateral modes have proved the validity of such an approach. They have opened a quest for an efficient, compact, spectrally resolving mode-reshaping photonic device. We expect that this photonic device will produce next-order-of-magnitude progress in single-mode power for laser diodes of various wavelengths and find its application in high-speed, high-power semiconductor sources.
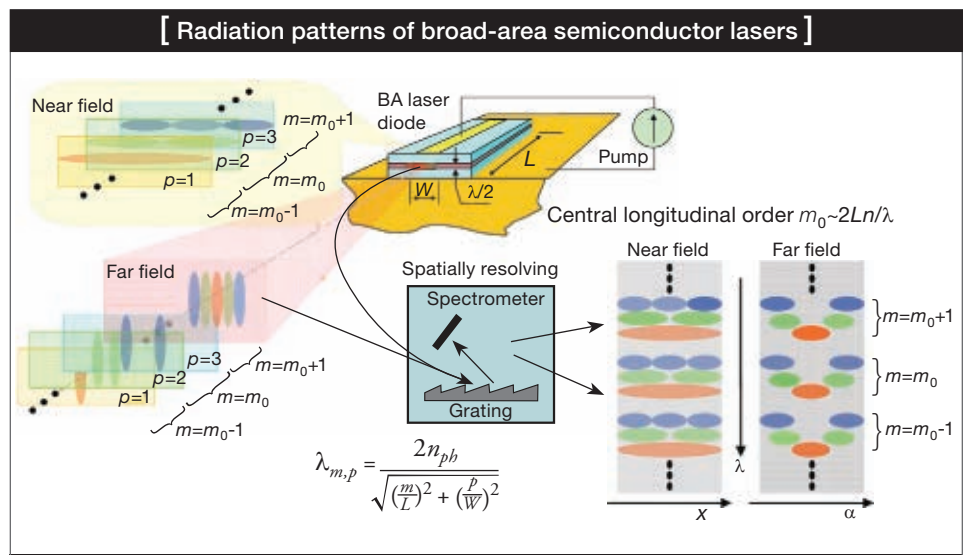
## Spatio-spectral structure of broad-area laser diode radiation

The combining methodology starts with understanding the fine modal structure of broad-area laser radiation. The cavity of edge-emitting lasers can be seen as a rectangular box of an optically transparent dielectric with refractive index $n$. The transversal (vertical) size is

typically chosen to provide single-mode operation, so that the vertical mode profile is the same for all modes. Therefore, the confinement in this direction is equivalent to an effective index, and the mode analysis can be reduced to a two-dimensional (lateral-longitudinal) plane. The simplified boundary conditions in the $x$-direction and the $z$-direction ($k_x = p\pi/W$, $k_z = m\pi/L$) restrict the angle and wavelength of the propagating wave inside the cavity of width $W$ and length $L$.

Each allowed propagating wave (mode) has specific longitudinal $m$ and lateral $p$ indices. The formula at the bottom of the figure below relates the $m$ and $p$ indices with the lasing wavelength. The rest of the figure shows the structure of the near and far fields of a broad-area laser. It also illustrates direct-mode visualization in a special spectrometer with spatial resolution. The top left portion of the figure shows the modal structure of the radiation at the output facet of the laser diode (near field). For the sake of simplicity, only three lateral modes are depicted.

Modes with different lateral indexes $p$ have different frequencies: A mode with a higher index has a shorter wavelength (within the same longitudinal order $m$); therefore, a mode with $p=1$ is shown as red; a mode with $p=2$ is shown as green; and a mode with $p=3$ is shown as blue. All modes are radiated from the same area $\approx W \times \lambda/2$ of the output facet. The near field has a corresponding angular distribution, or far field, that is depicted on the left lower side of the figure. The lateral modes are less spatially overlapped in the far field. Due to the periodic structure of the near field, the far field of each mode (except $p=1$) is represented by a two-peak pattern. The total output far field intensity profile is shown on the pink background. The lower right corner of the figure depicts spectrally resolved near- and far-field patterns that can be measured with a spatially resolving spectrometer. The approximate value of the central longitudinal order is given by the formula in the middle and yields a value of $2\times2\times3.3$ mm/0.001 mm = 13,200.



**[ Radiation patterns of broad-area semiconductor lasers ]**

Near field

BA laser diode

$p=3$
$p=2$
$p=1$

$m=m_0+1$
$m=m_0$
$m=m_0-1$

Pump

$W$  $\lambda/2$  $L$

Central longitudinal order $m_0 \sim 2Ln/\lambda$

Far field

$p=3$
$p=2$
$p=1$

$m=m_0+1$
$m=m_0$
$m=m_0-1$

Spatially resolving
Spectrometer

Grating

Near field     Far field

$\}m=m_0+1$
$\}m=m_0$
$\}m=m_0-1$

$x$     $\alpha$

$$\lambda_{m,p} = \frac{2n_{ph}}{\sqrt{(\frac{m}{L})^2 + (\frac{p}{W})^2}}$$

The wavelength-space spectrograms allow a quick visual analysis of a large number of modes—which is an important tool in combining techniques. In the simplest example, these spectra can be measured by a spectrometer collecting light from only a small part of the laser's output facet selected by a pinhole. By displacing the pinhole along the facet, one accumulates a series of spectra corresponding to different parts of the facet. The resulting intensity data have two coordinates: the spatial coordinate x and the wavelength λ.

The figure below illustrates the connection between these 3-D spatio-spectral-intensity measurements and conventional spectrally integrated near fields and spatially-integrated spectra. Three blue arrows show the three basic variations on this basic 3-D representation: 1) A spectrally integrated spatial profile (near field without spectral dispersion); this profile, for example, can be measured by moving a small photo-detector across the output facet of the diode; 2) A spectral view (right side arrow); this type of measurement is performed by a conventional spectrometer, but special care must be taken to assure that all spatial frequencies of radiation are collected; and 3) The third arrow shows a spatio-spectral density map (top view) that is increasingly becoming the method of choice for diode laser characterization. The intensity values are shown in gray or artificial color scales. Unlike the spatio-spectral views the spectrally integrated spatial profiles and spatially integrated spectral profiles do not uniquely identify the laser diode mode structure (i.e., the same profiles can be obtained from several different spatio-spectral maps, as shown in the lower left corner of the figure below).

Finally, the bottom right portion of the figure shows spectrally resolved near (NF) and (FF) far fields of laser diodes with three different geometries and manufacturing designs that are operating at the maximum output power. The three broad-area diode lasers are: 1) a 1-mm-long 98-µm-wide InGaAs laser with 1 W of output power at 980 nm; 2) a 2.4-mm-long, 94-µm-wide InGaAs single quantum well laser with 2 W of maximum power at 978 nm; 3) a 3.6-mm-long, 94-µm-wide laser with 4 W of output power at λ=945 nm. The threshold currents are 260, 300 and 320 mA, respectively. All spectra show qualitative agreement with the box model formula.

The measurements were done in a spatially and angularly resolving grating spectrometer with high spectral resolution. The figure depicts the central fragments from the near- and far-field spectra of all three laser diodes. As shown, at high power in two
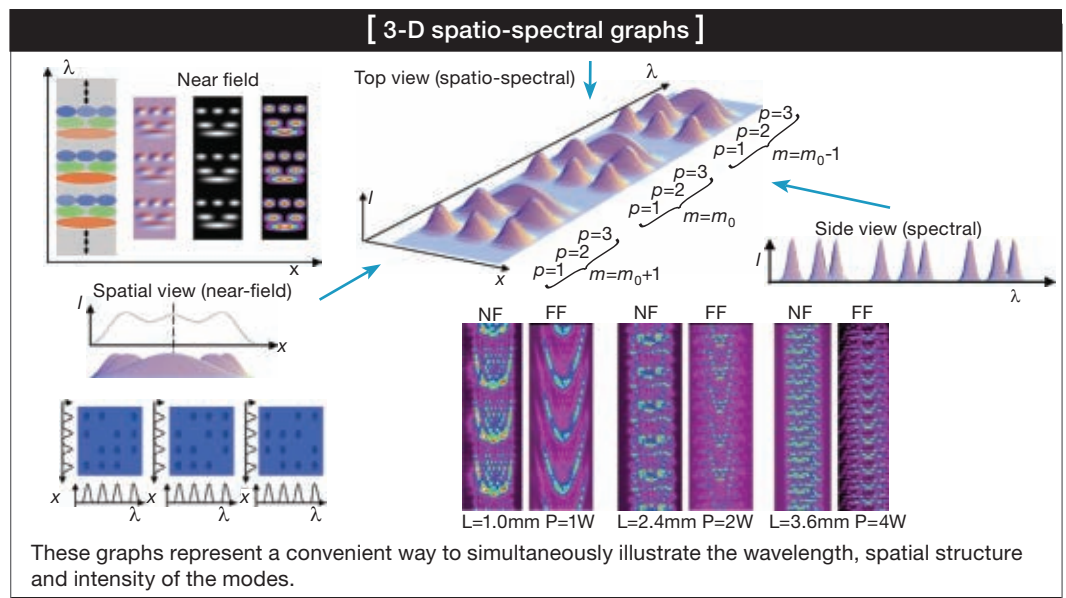
of the three lasers, the high-order lateral modes of one longitudinal group start to overlap in wavelength with the low-order lateral modes of another longitudinal group. The mode identification in the near field after such mode overlap is difficult and may be impossible. However, in the far field, mode positions are still distinguishable up to maximum power.

The study of angularly resolved (i.e., far-field) spectra have shown that all of the broad-area lasers that have been investigated to date demonstrate a well distinguishable and stable mode structure at the nominal power levels that corresponds to reliable laser operation [Proc. SPIE **7230**, 72301B (2009)]. Laser samples, regularly measured for more than two years, demonstrate no detectable spatial-spectral pattern variation.

## Lateral-mode combining for broad-area laser diodes

The key point of the combining concept is the following: If a laser has a stable mode structure and each mode has a distinct wavelength, each lateral mode can be spectrally isolated, individually reshaped into a single-lobe pattern and then re-combined into one spatially coherent beam with a theoretical efficiency of 100 percent. While the spectral dispersion and combining are common and well understood processes, the mode reshaping requires some introduction. Let us imagine that a high-order mode or a mixture of coherent modes arrives at the input of a black box. The refractive index variations inside of the black box can reshape the input mode into a fundamental one.

In the first experiments, a simple one-layer phase mask was used as the black-box transformer. The reshaping principle is similar to the focusing process by a Fresnel lens and can be easily understood in the simple example of a binary mask, as shown in the figure below and to the left on p. 24. The instantaneous snapshot of the input mode field is shown in violet.



[ 3-D spatio-spectral graphs ]

These graphs represent a convenient way to simultaneously illustrate the wavelength, spatial structure and intensity of the modes.

By applying the phase-inverting mask to the areas of the field profile with negative values, one can develop an entirely positive profile (pink color) that will have significant overlap with the profile of the fundamental mode (green dashed line).

This simple device, often called the phase-front "rectifier," creates a fully positive wavefront with 67 percent overlap with the fundamental mode. The double spatial frequency modulation of the wavefront, which is still present after "rectification," generates high-order beams in the far field and creates the unwanted scattering of energy. These high-order beams can be caught in a more sophisticated design with several phase masks. Ultimately, one can achieve a near-100 percent reshaping process in distributed optical structures realized in planar light-wave circuits or in volume phase masks.

Let us now reiterate the dispersion/combining steps. The spectral decomposition is done using high-efficiency diffraction gratings in a conventional 4-f spectrometer configuration. The initial demonstration of mode combining with two spatially resolving spectrometers that had opposite spectral dispersion and a phase mask in the spectral plane, is shown in the lower half of the figure below and to the right. The various longitudinal and lateral modes are resolved after projection onto the spectral plane. Then, each profile of the mode is individually modified by a phase modulating device. The modes are then spectrally recombined into a nearly single-mode profile and finally coupled to a single-mode fiber.
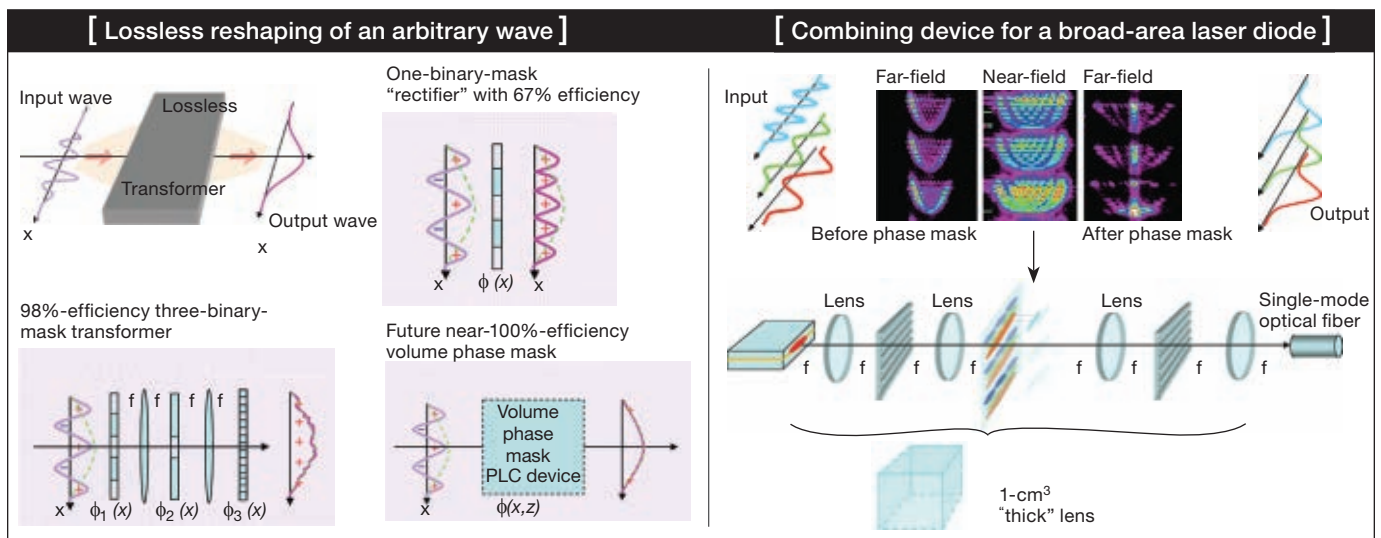
For the sake of simplicity, in this figure, we show only a one-layer binary phase mask modulator; however, all optical transformers discussed in the preceding figure on this page can be incorporated here after some straightforward modifications. The input optical system (depicted as the first lens) has a high numerical aperture (NA >0.5). Unfortunately, standard microscope objectives are not suitable for this task; they have a small working distance from the focal point to the first lens, and they typically provide strong optical feedback that practically destroys the intrinsic mode pattern of broad-area lasers. Long-working-distance objectives with good anti-reflective coating are used.

The system must have a sufficient spectral resolution to separate the closest modes. At moderate power, assuming only one longitudinal order, the frequency distance between mode $p$=1 and mode $p$=2 is the smallest one and equals approximately $\Delta f \approx (p_2^2 - p_1^2)[c\lambda_0/(8\ n^2\ W^2)] \approx 1$ GHz for 980 nm, 100-μm-wide lasers. The length of a diffraction grating with the same spectral resolution is equal to $L = c/(2\Delta f) \approx 15$ cm! We have implemented various multi-pass schemes to avoid using such long gratings. Due to the fact that the length $L$ scales linearly with the number of folded passes, and the total transmission scales exponentially, such a scheme transforms the length limitation into a length-efficiency trade-off : $L \ln(R) \approx L (1-R) \approx$ const, where $R$ is the cumulative reflectance of the multi-pass grating. Thus, if $R$ is close enough to 1, the significant reduction of grating size made by folding only slightly reduces the total efficiency of the combining system.

The fundamental mode passes through the system unchanged, but high-order modes acquire phase inversion of either odd or even peaks. Three photos in the upper center of the figure show the experimental measurements of spatially resolved near- and far-field spectra at the spectral plane of the combiner. Before and after application of the phase mask, the near-field power spectrum stays the same. However, the far field changes dramatically. The left spectrum shows the far field before the application of the phase mask and the right spectrum shows the far field after the phase mask. In the latter case, high-order parabolic tails have double spatial frequency.

In a folded version, the whole scheme has a size of 10×10× 150 cm³. We expect that using custom-made optical components and multiple-fold bulk or volume grating schemes can reduce the size of the combiner to about 1 cm³. For example, a 16×-folding scheme using gratings with dielectric coating of 99 percent reflectance reduces the total transmission from 99



[ Lossless reshaping of an arbitrary wave ]

Input wave
Lossless Transformer
Output wave

One-binary-mask "rectifier" with 67% efficiency

98%-efficiency three-binary-mask transformer

Future near-100%-efficiency volume phase mask

Volume phase mask PLC device
$\phi(x,z)$

[ Combining device for a broad-area laser diode ]

Input

Far-field    Near-field    Far-field

Before phase mask    After phase mask

Output

Lens    Lens    Lens    Single-mode optical fiber

1-cm³ "thick" lens

to 92–93 percent, while the grating length assuring 1 GHz resolution becomes smaller than 1 cm. An order-of-magnitude analysis, when completed with detailed arguments, predicts that a 85–90-percent-efficient compact combining/reshaping device is feasible in the near future.
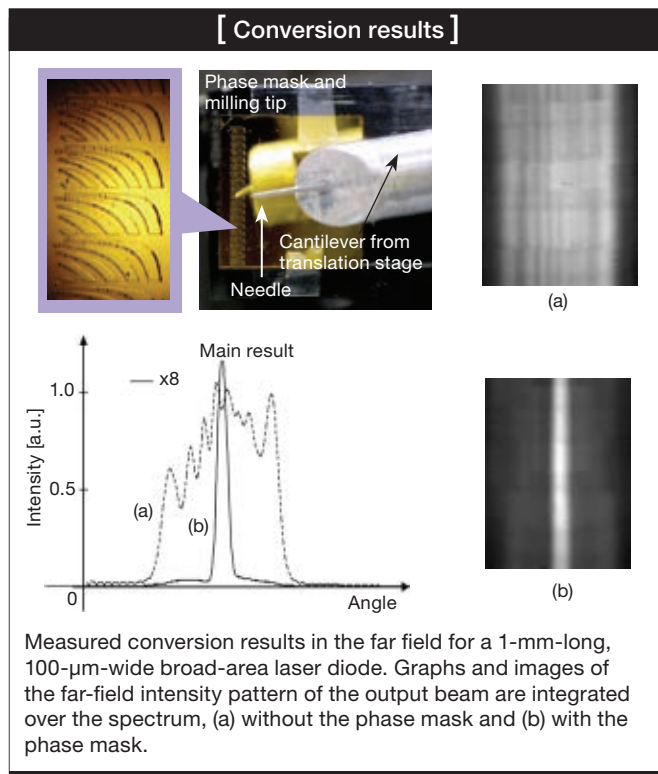
The initial demonstration described above implemented the combining procedure with off-the-shelf components. The total transmission of this system without a phase mask is 35–40 percent. The realization of the phase mask for 400 modes requires an automated phase-mask fabrication machine, implemented as follows. A high-resolution camera mounted on a calibrated precision translation stage, acquires a 2-D spatially resolved spectrum of laser modes. Mode peaks are automatically detected and a binary phase mask is generated by a simple algorithm. Using a mechanical tool (a sharp tip), a phase-inverting layer of photo-resist is removed in pre-calculated areas as shown in the figure on the right. Once the process is optimized, the mask-writing procedure takes only 10 min. for a 600-mode mask. When the phase mask is introduced into the optical path, the multimode laser light with wide angular spread is concentrated into a single diffraction-limited beam. For a laser with an output power of 120 mW, this experiment has demonstrated 60 percent photon-to-photon conversion efficiency.

For a non-overlapping modes situation of moderate power, the combining is expected to yield nearly 100 percent conversion efficiency. For high-power situations where some modes are overlapped in the spectrum or are frequency-degenerate and not phase-locked, the conversion efficiency will drop for these modes according to the degree of degeneracy. Preliminary numerical estimations using a box model of modes or experimentally measured spectra show only a slight loss of efficiency. This is due to the fact that degeneracy is still rare with two- and three-order overlap. In addition, other preliminary data show a mode competition and even phase lock between degenerate modes—which may eventually increase the total conversion efficiency. Following these arguments, it is reasonable to expect only a slight degradation of conversion efficiency at high power and expect 60 to 80 percent efficient devices for multimode broad-area lasers. With inexpensive broad-area devices, this value of efficiency is very attractive when we consider the possibility of having directly modulated beams with tens of watts of spatially coherent power.

## Future perspectives

We believe that nothing prevents one from reshaping the radiation of a broad area laser into a spatially single-mode spot, except for the apparent complexity of the external optical device. The initial simple proof-of-concept experimental results can be significantly improved by using low-loss and integrated-optical components. These same principles can be extended to various laser geometries and wavelengths, and to quantum cascade lasers in particular.

These mode transformation methods can also find application in the low-noise optical amplification of images, where the input signal modes must be reshaped into amplifier-specific modes.



**[ Conversion results ]**

Main result

Measured conversion results in the far field for a 1-mm-long, 100-µm-wide broad-area laser diode. Graphs and images of the far-field intensity pattern of the output beam are integrated over the spectrum, (a) without the phase mask and (b) with the phase mask.

Looking forward, we can mention the further development of practical unitary phase transformers with nearly 100 percent efficiency; this would potentially merge the phase mask reshaping and spectral selection operations in one photonic-crystal-like device.

Thus, if the engineering of reducing the size, loss and cost of the mode combiner is mastered, such a combining device can be a part of a standard broad-area laser module—and, this may broaden the scope of applications for semiconductor lasers. ▲

**Nikolai Stelmakh** (nikolais@uta.edu) and **Michael Vasilyev** are with the department of electrical engineering at the University of Texas at Arlington, Arlington, Texas, U.S.A.

**[ References and Resources ]**

>> J.K. Butler and H. Kressel. *Semiconductor Lasers and Heterojunction LEDs*. Chap. 6 and 7, Academic Press, 1977.

>> G.A. Evans and J.M. Hammer. Academic Press, 1993.

>> K. Petermann. IEEE J. Sel. Topics in Quantum Electron. **1**, 480–9 (1995).

>> D.F. Welch. IEEE J. of Sel. Topics in Quantum Electron. **6**, 1470–7 (2001).

>> N. Stelmakh and M. Flowers. Photon. Technol. Lett. **18**, 1618–20 (2006).

>> N. Stelmakh. Photon. Technol. Lett. **19**, 1392–4 (2007).

>> J.J. Lim et al. IEEE J. of Sel. Topics in Quantum Electron. **15**, 993–1008 (2009).

>> V. Stelmakh and N. Stelmakh. FiO/LS paper JSuA29, San Jose (September 2007).

>> N. Stelmakh et al. Appl. Phys. Lett. **94**, 013501 (2009).

>> N. Stelmakh. Proc. SPIE **7230**, 72301B (2009).

>> M. Vasilyev et al. Opt. Express **17**, 11415 (2009).